Eur. Phys. J. Spec. Top. (2022) 231:4057–4064
https://doi.org/10.1140/epjs/s11734-022-00691-7

THE EUROPEAN PHYSICAL JOURNAL SPECIAL TOPICS

Regular Article

Synchronization in a network of map-based neurons with memristive synapse

Zhen Wang[1,2], Huaigu Tian[1], Ondrej Krejcar[3,4,5], and Hamidreza Namazi[6,3,a]

[1] Xi'an Key Laboratory of Human-Machine Integration and Control Technology for Intelligent Rehabilitation, School of Computer Science, Xijing University, Xi'an 710123, People's Republic of China
[2] Xi'an Key Laboratory of Advanced Photo-Electronics Materials and Energy Conversion Device, School of Electronic Information, Xijing University, Xi'an 710123, People's Republic of China
[3] Faculty of Informatics and Management, Center for Basic and Applied Research, University of Hradec Kralove, Hradec Králové, Czechia
[4] Institute of Technology and Business in Ceske Budejovice, Ceske Budejovice, Czechia
[5] Malaysia Japan International Institute of Technology (MJIIT), Universiti Teknologi Malaysia, Kuala Lumpur, Malaysia
[6] School of Engineering, Monash University, Subang Jaya, Selangor, Malaysia

Received 15 August 2022 / Accepted 27 September 2022 / Published online 25 October 2022

Abstract The synchronization of coupled neurons has been an important field of study in neuroscience. In this paper, the synchronization in coupled map-based neurons is studied. It is assumed that the neurons are coupled via a memristor. Firstly, the case of two-coupled neurons is investigated, and then two neurons are used as the units of a ring network. It is shown that the memristive coupling coefficient and the initial condition of the flux variable affect the synchronization of two neurons. By increasing the memristive coupling coefficient, multiple synchronous and asynchronous regions are observed. In the ring network, two neurons in each unit can become synchronous, but the whole network does not reach complete synchronization.

1 Introduction

Synchronization is a critical collective behavior in coupled dynamical systems [1]. In general, synchronization is associated with different phenomena in various sciences, such as physics, neuroscience, ecology, etc. [2, 3]. Synchronization of chaotic systems has attracted much attention in recent years [4–6]. In neuroscience, synchronization has many relations with the natural brain function, such as cognitive tasks [7]. Therefore, it has been remarkably studied in various neuronal networks with different neuron models, network structures, and coupling schemes [8–10].

Most studies on the synchronization of the neurons have been done on the flow models [11–13]. In these studies, continuous-time neuron models, such as Hodgkin–Huxley, Hindmarsh–Rose, Fitzhugh–Nagumo, etc., have been used. For example, Sun et al. [13] considered a network of subnetworks consisting of Hindmarsh–Rose neurons and showed two types of burst synchronizations. Nikitin et al. [14] studied partial synchronization patterns in a multiplex network of FitzHugh–Nagumo oscillators with delayed coupling. Shafiei et al. [15] investigated the coupled Izhikevich neurons with partial time delay. They reported the effect of the partial time delay on the level of synchronization and also on the formation of different spatiotemporal patterns. The synchronization has also been studied in non-identical neurons. For example, Yao et al. [16] focused on the possibility of the occurrence of synchronization in two photosensitive and thermosensitive neurons.

In addition to the ordinary differential equations (ODEs), some discrete dynamical systems (maps) have been introduced that can represent the biological dynamics of the neurons [17]. Discretization of ODEe has been used widely in different complex systems. Using map-based models decreases the computational cost significantly. Hence, some studies focusing on synchronization have employed map-based neuron models [18–20]. Tanaka et al. [18] studied the in-phase and antiphase synchronization in a network of map-based bursting neurons. Rakshit et al. [21] investigated the dynamics of two-coupled neuronal Rulkov maps with chemical synaptic interactions. The effects of the time delay and

Collective Behavior of Nonlinear Dynamical Oscillators. Guest editors: Sajad Jafari, Bocheng Bao, Christos Volos, Fahimeh Nazarimehr, Han Bao.

[a] e-mail: Hamidreza.namazi@monash.edu (corresponding author)

autapse were also under consideration. Sausedo-Solorio and Pisarchik [22] considered the Rulkov maps with memory and synaptic delay and observed lag or anticipated synchronization. The network of the memristive version of the Rulkov model was studied by Mehrabbeik et al. [23]. They showed that in contrast to the original Rulkov models, two electrically coupled memristive Rulkov maps could reach complete synchronization.

In recent years, memristors have found significant applications in chaotic systems [24–26]. Different firing patterns in neurons can lead to the induction of electromagnetic fields, which can be considered by the memristive coupling between neurons [27–29]. Bao et al. [27] reported coexisting firing patterns in two neurons coupled with a memristor with the threshold memductance. Different coherent and incoherent spatiotemporal patterns, such as the chimera state [30], have also been found in memristive coupled neurons [31]. In this paper, we consider KTz map-based neuron models with memristive coupling. Memristive synapse can be a better model for the synapse plasticity. To the best of our knowledge, the synchronization of this model has not been studied before. The synchronization is studied by considering two-memristive-coupled neurons and a ring network of two neurons. The effects of varying the parameters of the coupling and memristor are investigated.

2 Model

The KT model is a two-dimensional map-based neuron model wherein a hyperbolic tangent function is used for modeling the membrane potential [32]. This original model has been extended by adding a third variable as the slow variable to be able to represent various bursting and spiking patterns (KTz model) [33]. To increase the computational efficacy of the KTz model, Girardi-Schappo et al. [34] modified this model by approximating the hyperbolic tangent function with a logistic function. This paper uses the modified KTz model for each neuron.

The following equations define the three-dimensional KTz map model:

$$\begin{aligned} x(t+1) &= f\left(\frac{x(t) - Ky(t) + z(t) + H + I(t)}{T}\right), \\ y(t+1) &= x(t), \\ z(t+1) &= (1-\delta)z(t) - \lambda(x(t) - x_R), \end{aligned} \tag{1}$$

where the gain function f is a hyperbolic tangent that by first-order expansion can be approximated with a logistic function:

$$f(u) = \frac{u}{1+|u|}. \tag{2}$$

In these equations, x is the membrane potential variable, y is the recovery variable, z is the slow current, and I denotes the external current. By appropriately adjusting the parameters, this map-based neuron model can represent different firing patterns, such as fast, slow, tonic, cardiac, phasic spiking, and bursting. Here, the parameters are set such that the neuron shows slow spiking behavior, $K = 0.6$, $T = 0.21$, $\delta = 0.01$, $\lambda = 0.01$, $x_R = -0.37$, $H = 0$. This behavior is shown in Fig. 1 for the initial conditions $(x_0, y_0, z_0) = (0, 0, 0)$.

When two neurons become connected through synapses, the information can be exchanged. Here, it is considered that the synaptic connection is via the memristor. The schematic of two neurons connected with a memristor is shown in Fig. 2. The current generating from the memristor can be described by:

Fig. 1 The schematic of two-coupled map-based neurons with memristive coupling

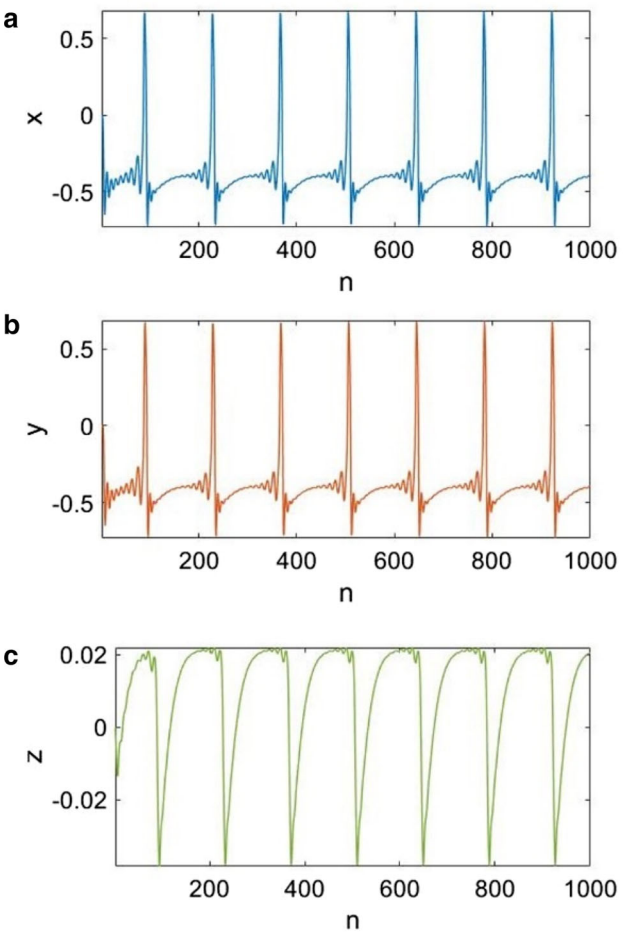

Fig. 2 The firing of the map-based neuron for $K = 0.6$, $T = 0.21$, $\delta = 0.01$, $\lambda = 0.01$, $x_R = -0.37$, $H = 0$. The initial condition is $(0, 0, 0)$

$$I_m = \rho(\phi)(x_1 - x_2)$$
$$\phi(t+1) = (x_1 - x_2) - \eta\phi(t) \quad (3)$$

where $\rho(\phi) = \alpha + 3\beta\phi^2$ is the memductance function of the memristor [35], and ϕ is the inner flux variable. Based on these definitions, two map-based neurons connected by a memristor can be described by:

$$\begin{aligned}
x_1(t+1) &= f\left(\frac{x_1(t) - Ky_1(t) + z_1(t) + H + I(t)}{T}\right) + \epsilon I_m,\\
y_1(t+1) &= x_1(t),\\
z_1(t+1) &= (1-\delta)z_1(t) - \lambda(x_1(t) - x_R),\\
x_2(t+1) &= f\left(\frac{x_2(t) - Ky_2(t) + z_2(t) + H + I(t)}{T}\right) - \epsilon I_m,\\
y_2(t+1) &= x_2(t),\\
z_2(t+1) &= (1-\delta)z_2(t) - \lambda(x_2(t) - x_R),\\
\phi(t+1) &= (x_1 - x_2) - \eta\phi(t),
\end{aligned} \quad (4)$$

where ϵ shows the memristor coupling coefficient between two neurons and η is the induction coefficient. The memductance function is considered as ρ with the parameters $\alpha = 0.1$ and $\beta = 0.03$.

This memristive coupling can lead to synchronized dynamics between neurons. To measure the synchronization between two neurons, the average synchronization error is calculated:

$$E = \langle\sqrt{(x_1 - x_2)^2 + (y_1 - y_2)^2 + (z_1 - z_2)^2}\rangle_t. \quad (5)$$

In addition to two-coupled neurons, the synchronization is investigated in a ring network of memristive coupled neurons. The schematic of this network is shown in Fig. 3. It should be noted that the ring of memristive coupled neurons is similar to a two-layer network with memristive interlayer couplings. Considering each two-coupled neuron as a subnetwork, a ring of subnetworks is constructed. This network can be described by:

$$\begin{aligned}
x_{1,i}(t+1) &= f\left(\frac{x_{1,i}(t) - Ky_{1,i}(t) + z_{1,i}(t) + H + I(t)}{T}\right)\\
&\quad + \epsilon\rho(\phi_i)(x_{1,i}(t) - x_{2,i}(t))\\
&\quad + \sigma(x_{1,i+1}(t+1) + x_{1,i-1}(t+1) - 2x_{1,i}(t+1)),\\
y_{1,i}(t+1) &= x_{1,i}(t),\\
z_{1,i}(t+1) &= (1-\delta)z_{1,i}(t) - \lambda(x_{1,i}(t) - x_R),\\
x_{2,i}(t+1) &= f\left(\frac{x_{2,i}(t) - Ky_{2,i}(t) + z_{2,i}(t) + H + I(t)}{T}\right)\\
&\quad - \epsilon\rho(\phi_i)(x_{2,i}(t) - x_{1,i}(t))\\
&\quad + \sigma(x_{2,i+1}(t+1) + x_{2,i-1}(t+1) - 2x_{2,i}(t+1)),\\
y_{2,i}(t+1) &= x_{2,i}(t),\\
z_{2,i}(t+1) &= (1-\delta)z_{2,i}(t) - \lambda(x_{2,i}(t) - x_R),\\
\phi_i(t+1) &= (x_{1,i}(t) - x_{2,i}(t)) - \eta\phi_i(t),
\end{aligned} \quad (6)$$

where σ shows the coupling strength between the subnetworks. Now, the synchronization error can be computed among the first neurons (E_1), or the second neurons (E_2) or among the first and second neurons in all subnetworks (E) as:

$$E_1 = \left\langle \frac{1}{N-1}\sum_{i=2}^{N}\sqrt{(x_{1,1}-x_{1,i})^2 + (y_{1,1}-y_{1,i})^2 + (z_{1,1}-z_{1,i})^2}\right\rangle_t \quad (7)$$

$$E_2 = \left\langle \frac{1}{N-1}\sum_{i=2}^{N}\sqrt{(x_{2,1}-x_{2,i})^2 + (y_{2,1}-y_{2,i})^2 + (z_{2,1}-z_{2,i})^2}\right\rangle_t \quad (8)$$

$$E = \left\langle \frac{1}{N}\sum_{i=1}^{N}\sqrt{(x_{1,i}-x_{2,i})^2 + (y_{1,i}-y_{2,i})^2 + (z_{1,i}-z_{2,i})^2}\right\rangle_t. \quad (9)$$

3 Results

At first, two map-based neurons with a memristive synapse are investigated. The synchronization error of two neurons is computed by varying the memristor coupling coefficient (ϵ) and the induction coefficient (η). The synchronization error between two neurons is shown in Fig. 4a. It can be observed that, generally, the synchronization is not dependent on the induction coefficient. In contrast, the memristor coupling coefficient plays an important point. However, its relation is not linear (see Fig. 4b). In fact, for small coupling coefficients, the neurons are asynchronous. For the small range $0.11 < \epsilon < 0.13$, the synchronization appears. By more increasing this coefficient, the synchronization is disturbed and again appears in the range $0.41 < \epsilon < 0.47$. An increment of the coupling coefficient from $\epsilon = 0.47$ leads to asynchronization, and finally, the neurons become synchronous for $\epsilon > 0.54$. The time series of the neurons for some different memristor coupling coefficients and induction coefficients are shown in Fig. 4c–f. The synchronous and asynchronous firing of neurons can be observed in these figures. It is seen that in the asynchronization mode, the subthreshold oscillations have some differences.

Investigating two neurons for different sets of initial conditions shows that another important parameter in the synchronization of two neurons is the initial condition of the flux variable. Thus, we calculate the synchronization error by varying the initial condition of the flux variable (ϕ_0) and the memristor coupling coefficient (ϵ). The result is shown in Fig. 5a. The black regions in this figure represent the instability of the neurons. It is observed that for $\phi_0 < -3.6$ and $\phi_0 > 7.2$, there is only one synchronization region, and the neurons become unstable for higher coupling coefficients. Out of this range, there are multiple synchronization regions by increasing ϵ. For example, the synchronization errors for $\phi_0 = -7, -4, 0, 7$ are shown in Fig. 5b–e. For $\phi_0 = -7$, the synchronization happens for $\epsilon > 0.02$, and for $\epsilon > 0.175$, the neurons become

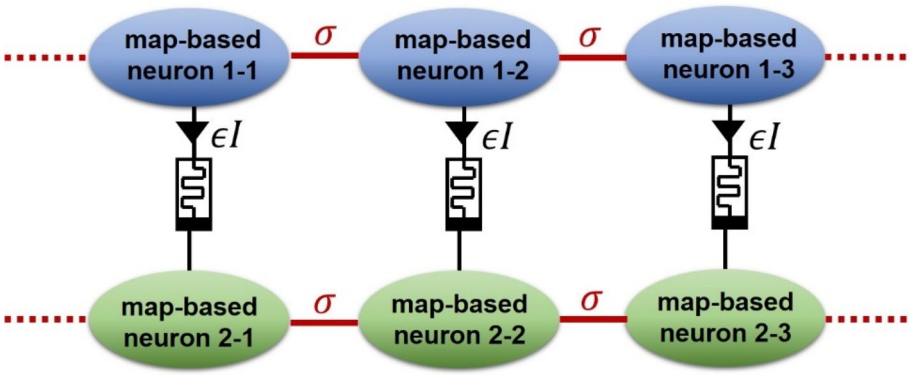

Fig. 3 The schematic of the ring network of two-memristive-coupled neurons. The memristor coupling coefficient is ϵ, and the coupling between subnetworks is shown by σ

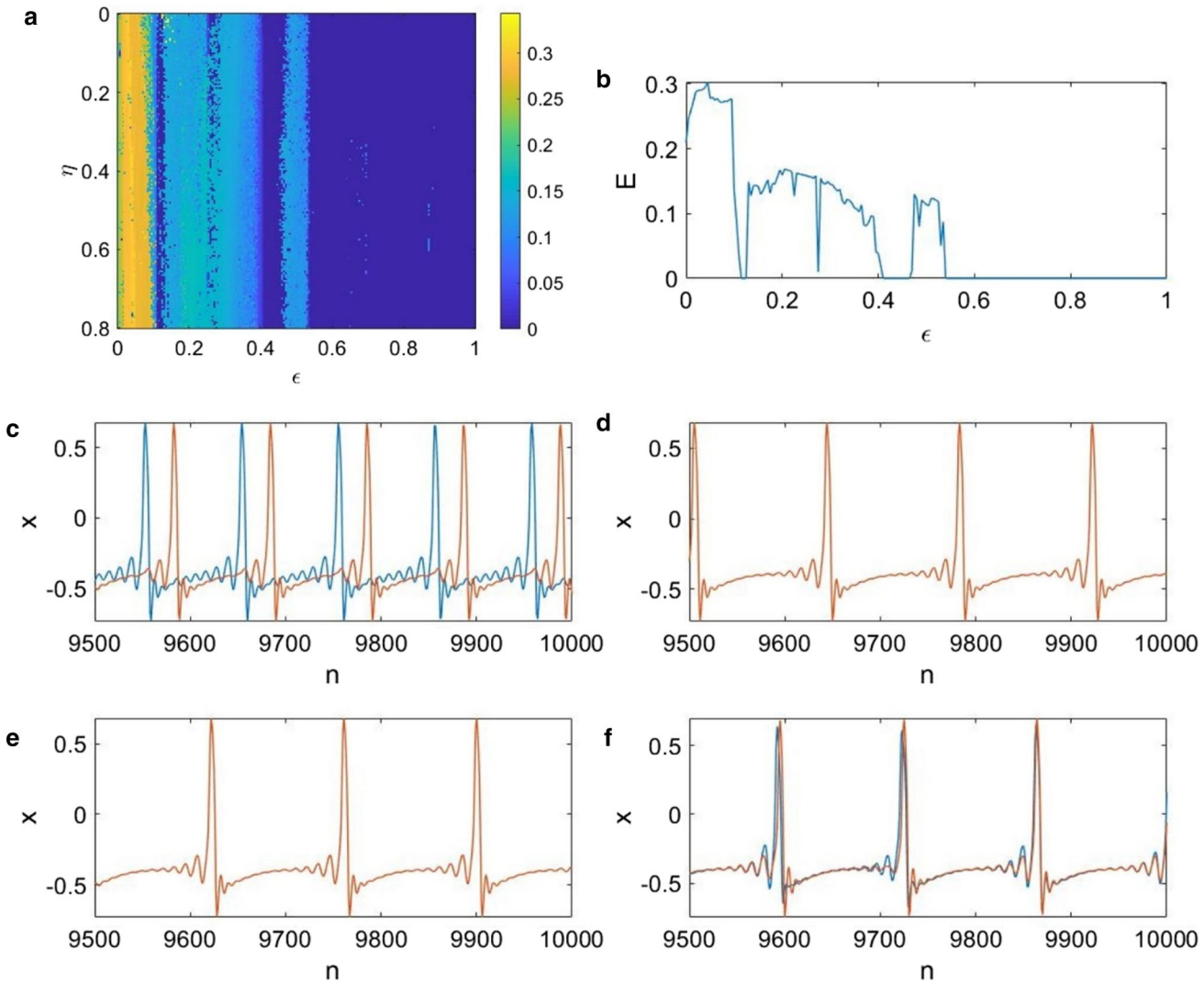

Fig. 4 **a** The result of synchronization error of two-memristive-coupled neurons by varying the memristor coupling coefficient (ϵ) and the induction coefficient (η). **b** The error for $\eta = 0.8$ with respect to ϵ. **c**–**f** The time series of two neurons for different η and ϵ: **c** $\eta = 0.1$, $\epsilon = 0.05$, **d** $\eta = 0.1$, $\epsilon = 0.6$, **e** $\eta = 0.5$, $\epsilon = 0.6$, **f** $\eta = 1$, $\epsilon = 0.5$. The initial conditions are [0.91 0.91 0.1 0.55 0.96 0.97 5]

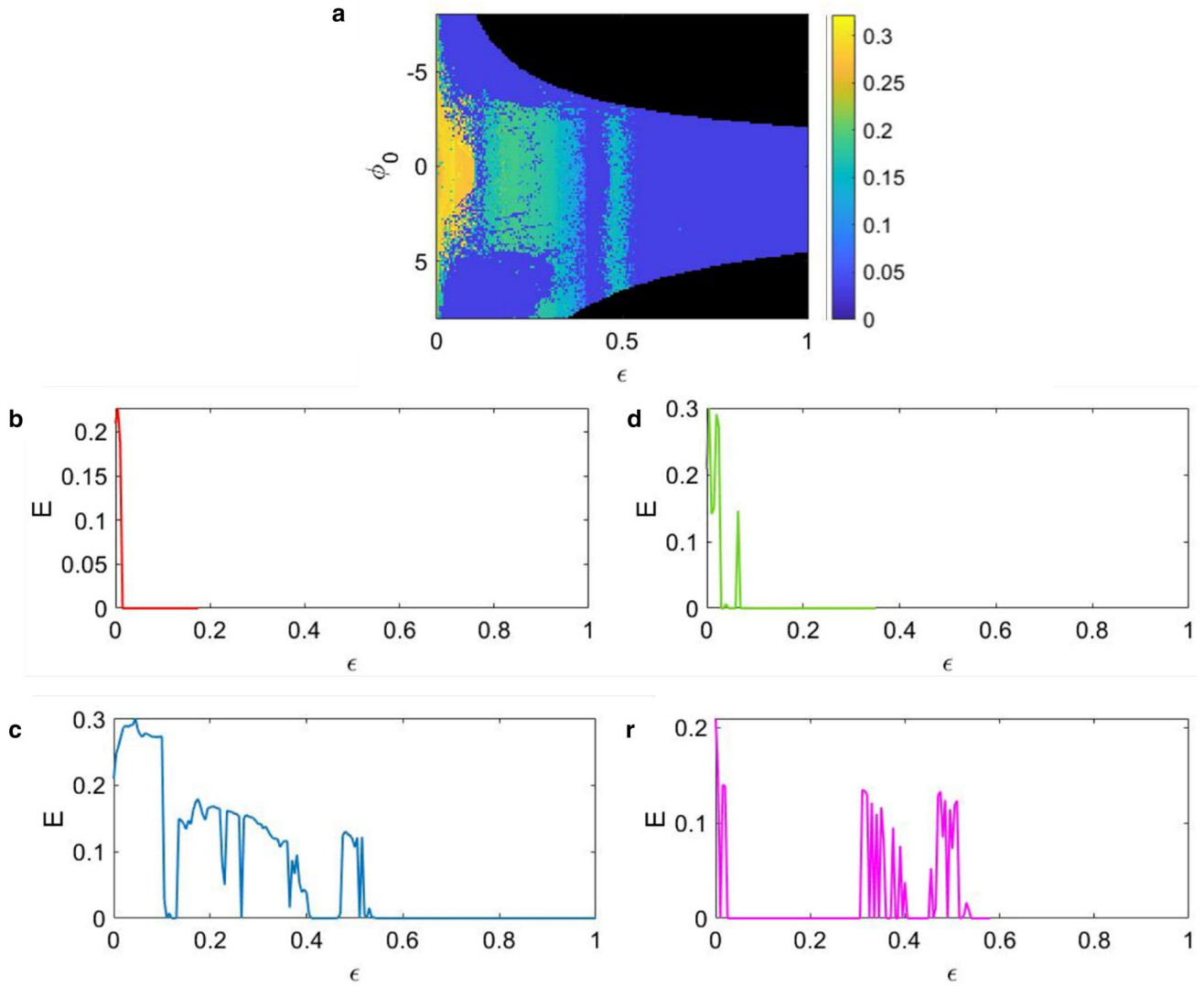

Fig. 5 **a** The result of synchronization error of two-memristive-coupled neurons by varying the memristor coupling coefficient (ϵ) and the initial condition of the flux variable (ϕ_0). The color represents the synchronization error and the black shows the instability region. **b**–**e** The error with respect to ϵ for $\phi_0 = -7$, $\phi_0 = -4$, $\phi_0 = 0$, $\phi_0 = 7$. The initial conditions are the same as Fig. 4

unstable. For $\phi_0 = -4$, there is a narrow synchronization region in $0.03 < \epsilon < 0.06$, and then the neurons become synchronous at $\epsilon > 0.08$. The instability occurs for $\epsilon > 0.35$. For $\phi_0 = 0$, there are multiple synchronization regions in $0.11 < \epsilon < 0.13$, $0.41 < \epsilon < 0.47$, and $\epsilon > 0.54$. The neurons do not become unstable in this case. For $\phi_0 = 7$, there is a large synchronization region in $0.025 < \epsilon < 0.3$ and a small synchronization region in $0.4 < \epsilon < 0.45$, and instability occurs at $\epsilon = 0.58$. Therefore, the value of the initial flux variable is significant in the synchronous firing of two neurons.

Next, the memristive synapse coupled neurons are considered as the subnetworks of a ring network (Fig. 3), and their synchronization is studied. The synchronization error is computed among the first neurons, among the second neurons, and the first and second neurons in all subnetworks. These synchronizations are calculated by varying the coupling between subnetworks (σ) and the memristive coupling coefficient (ϵ). As it was shown that the initial condition of the flux variable is an essential factor, we consider four different values for this variable as $\phi_0 = -6.2, -2.2, 2, 7.8$. The results are shown in Fig. 6. In this figure, the left column shows the error of all first and second neurons (E), the middle column shows the error of the first neurons (E_1), and the right column shows the error of the second neurons (E_2). The dark blue region represents the synchronization region, and the black shows instability. The first column shows that the first and second neurons in subnetworks can become synchronous in an area of σ and ϵ. According to the middle column (and the right column), all of the first neurons of subnetworks (and the second neurons of subnetworks)

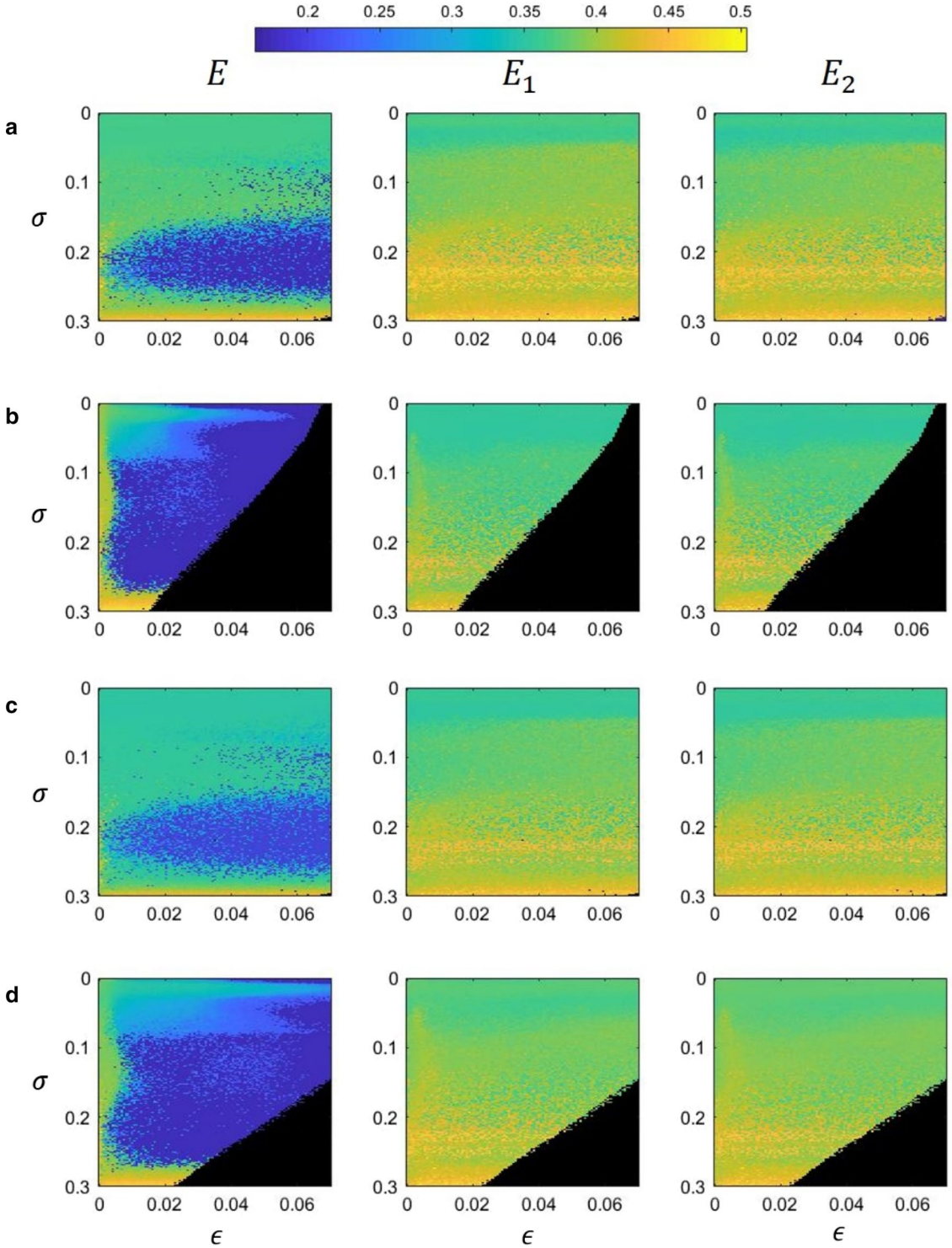

Fig. 6 The synchronization errors of the ring network by varying σ and ϵ. Left column: The error of the first and second neurons in all subnetworks, middle column: the error of the first neurons, right column: the error of the second neurons. **a** $\phi_0 = 2$, **b** $\phi_0 = 7.8$, **c** $\phi_0 = -2.2$, **d** $\phi_0 = -6.2$. The color represents the synchronization error and the black shows the instability region

are asynchronous in this region. This means that two-memristive-coupled neurons are synchronous, but the subnetworks cannot become synchronous. Furthermore, this region is wider for larger ϕ_0 values (see parts b and d in the left column). However, the instability region also exists in larger ϕ_0 values and increases by increasing ϕ_0.

4 Conclusion

This paper investigated the synchronization of map-based neurons with memristor synapse. At first, two neurons coupled with a memristive synapse were considered. The synchronization error of two neurons was computed by varying the memristor coupling coefficient and the induction coefficient. It was observed that the synchronization depends only on the memristor coupling coefficient. In fact, by increasing the memristor coupling coefficient, multiple synchronous and asynchronous regions were formed. Furthermore, the effect of the initial conditions was studied, and it was revealed that the initial condition of the flux variable has an essential role in the synchronization of neurons. As the initial condition of the flux variables was increased, the instability region happened in lower coupling coefficients. A ring network of two-memristive coupled neurons was studied in the next step. Three synchronization errors were computed: error among the first and second neurons in all units, the error among the first neurons, and the error among the second neurons. The results showed that the first and second neurons in the subnetworks could become synchronous for particular coupling coefficients. But the synchronization could not occur in all units.

Acknowledgements The author acknowledges the referees and the editor for carefully reading this paper and giving many helpful comments. This work is supported by the Natural Science Basic Research Program of Shaanxi (2021JM-533, 2021JQ-880, 2020JM-646), the Innovation Capability Support Program of Shaanxi (2018GHJD-21), the Science and Technology Program of Xi'an (2019218414GXRC020CG021-GXYD20.3), the Support Plan for Sanqin Scholars Innovation Team in Shaanxi Province of China, the Scientific Research Program Funded by Shaanxi Provincial Education Department (21JK0960), the Youth Innovation Team of Shaanxi Universities and the Scientific Research Foundation of Xijing University (XJ21B01), the Scientific Research Foundation of Xijing University (XJ210203), Long Term Development Plan of Research Organization, Institute of Technology and Business in Ceske Budejovice, Czech Republic, Project (2022/2204), Grant Agency of Excellence, University of Hradec Kralove, Faculty of Informatics and Management, Czech Republic.

Funding Information Open Access funding enabled and organized by CAUL and its Member Institutions.

Data availability statement Data sharing not applicable to this article as no datasets were generated or analyzed during the current study.

References

1. S. Boccaletti, A.N. Pisarchik, C.I. Del Genio, A. Amann, *Synchronization: From Coupled Systems to Complex Networks* (Cambridge University Press, Cambridge, 2018)
2. F. L. Lewis, H. Zhang, K. Hengster-Movric, A. Das, in *Cooperative Control of Multi-Agent Systems* (Springer, Berlin, 2014), pp. 1–21
3. B. Blasius, A. Huppert, L. Stone, Nature **399**, 354–359 (1999)
4. M. Paul Asir, K. Sathiyadevi, P. Philominathan, D. Premraj, Chaos **32**, 073125 (2022)
5. V. Sundarapandian, R. Karthikeyan, Eur. J. Sci. Res. **64**, 94–106 (2011)
6. K. Ponrasu, K. Sathiyadevi, V. Chandrasekar, M. Lakshmanan, EPL (Europhys. Lett.) **124**, 20007 (2018)
7. P.J. Uhlhaas, W. Singer, Neuron **52**, 155–168 (2006)
8. A. Bahramian, F. Parastesh, V.-T. Pham, T. Kapitaniak, S. Jafari, M. Perc, Chaos **31**, 033138 (2021)
9. Z. Wang, R. Ramamoorthy, X. Xi, K. Rajagopal, P. Zhang, S. Jafari, Eur. Phys. J. Spec. Top. (2022). https://doi.org/10.1140/epjs/s11734-022-00558-x
10. D. Eytan, S. Marom, J. Neurosci. **26**, 8465–8476 (2006)
11. Y. Xu, Y. Jia, J. Ma, A. Alsaedi, B. Ahmad, Chaos Solitons Fractals **104**, 435–442 (2017)
12. J. Ma, F. Wu, C. Wang, Int. J. Mod. Phys. B **31**, 1650251 (2017)
13. X. Sun, J. Lei, M. Perc, J. Kurths, G. Chen, Chaos **21**, 016110 (2011)
14. D. Nikitin, I. Omelchenko, A. Zakharova, M. Avetyan, A.L. Fradkov, E. Schöll, Philos. Trans. R. Soc. A **377**, 20180128 (2019)
15. M. Shafiei, F. Parastesh, M. Jalili, S. Jafari, M. Perc, M. Slavinec, Eur. Phys. J. B **92**, 1–7 (2019)
16. Z. Yao, P. Zhou, Z. Zhu, J. Ma, Neurocomputing **423**, 518–534 (2021)
17. B. Ibarz, J.M. Casado, M.A. Sanjuán, Phys. Rep. **501**, 1–74 (2011)
18. G. Tanaka, B. Ibarz, M.A. Sanjuan, K. Aihara, Chaos **16**, 013113 (2006)
19. X. Shi, Q.J.P.A.S.M. Lu, Physica A **388**, 2410–2419 (2009)
20. D. Hu, H. Cao, Commun. Nonlinear Sci. Numer. Simul. **35**, 105–122 (2016)
21. S. Rakshit, A. Ray, B.K. Bera, D. Ghosh, Nonlinear Dyn. **94**, 785–805 (2018)
22. J. Sausedo-Solorio, A. Pisarchik, Phys. Lett. A **378**, 2108–2112 (2014)

23. M. Mehrabbeik, F. Parastesh, J. Ramadoss, K. Rajagopal, H. Namazi, S. Jafari, Math. Biosci. Eng. **18**, 9394–9409 (2021)
24. D. Premraj, S. Kumarasamy, K. Thamilmaran, K. Rajagopal, Eur. Phys. J. Spec. Top. (2022). https://doi.org/10.1140/epjs/s11734-022-00562-1
25. P. Durairaj, S. Kanagaraj, T. Kathamuthu, K. Rajagopal, Int. J. Bifurc. Chaos **32**, 2230022 (2022)
26. K. Rajagopal, A. Bayani, A.J.M. Khalaf, H. Namazi, S. Jafari, V.-T. Pham, AEU Int. J. Electron. Commun. **95**, 207–215 (2018)
27. B. Bao, Q. Yang, D. Zhu, Y. Zhang, Q. Xu, M. Chen, Nonlinear Dyn. **99**, 2339–2354 (2020)
28. C. Chen, J. Chen, H. Bao, M. Chen, B. Bao, Nonlinear Dyn. **95**, 3385–3399 (2019)
29. Q. Xu, X. Tan, D. Zhu, M. Chen, J. Zhou, H. Wu, Math. Probl. Eng. **2020**, 8218740 (2020)
30. F. Parastesh, S. Jafari, H. Azarnoush, Z. Shahriari, Z. Wang, S. Boccaletti, M. Perc, Phys. Rep. **898**, 1–114 (2021)
31. H. Bao, Y. Zhang, W. Liu, B. Bao, Nonlinear Dyn. **100**, 937–950 (2020)
32. O. Kinouchi, M.H. Tragtenberg, Int. J. Bifurc. Chaos **6**, 2343–2360 (1996)
33. S.M. Kuva, G.F. Lima, O. Kinouchi, M.H. Tragtenberg, A.C. Roque, Neurocomputing **38**, 255–261 (2001)
34. M. Girardi-Schappo, G.S. Bortolotto, R.V. Stenzinger, J.J. Gonsalves, M.H. Tragtenberg, PLoS One **12**, e0174621 (2017)
35. M. Lv, C. Wang, G. Ren, J. Ma, X. Song, Nonlinear Dyn. **85**, 1479–1490 (2016)